Studying the "Underlying Event" in Drell-Yan and High Transverse Momentum Jet Production at the Tevatron

Rick Field and Deepak Kar
Department of Physics, University of Florida
Gainesville, Florida, 32611, USA

and

Craig Group
Fermilab, P.O. Box 500
Batavia, IL 60510-5011, USA

February 1, 2009 (Version 1)

Abstract

We study the behavior of charged particles ($p_T > 0.5$ GeV/c, $|\eta| < 1$) produced in association with Drell-Yan lepton-pairs in the region of the Z-boson ($70 < M(pair) < 110$ GeV/c^2) in proton-antiproton collisions at 1.96 TeV. We also study the behavior of charged particles ($p_T > 0.5$ GeV/c, $|\eta| < 1$) produced in association with large transverse momentum jets. We use the direction of the Z-boson (in Drell-Yan production) or the leading jet (in high p_T jet production) in each event to define three regions of η-ϕ space; "toward", "away", and "transverse". For Drell-Yan production (excluding the leptons) both the "toward" and "transverse" regions are very sensitive to the "underlying event". In high p_T jet production the "transverse" region is very sensitive to the "underlying event" and is separated into a MAX and MIN "transverse" region, which helps separate the "hard component" (initial and final-state radiation) from the "beam-beam remnant" and multiple parton interaction components of the scattering. For Z-boson production the average charged particle transverse momentum is plotted versus the charged particle multiplicity (excluding the leptons). The rate of change of $\langle p_T \rangle$ versus charged multiplicity is a measure of the amount of hard versus soft processes contributing and it is sensitive the modeling of the multiple-parton interactions. The data are corrected to the particle level and are then compared with several PYTHIA models (with multiple parton interactions) and HERWIG (with and without multiple parton interactions) at the particle level (*i.e.* generator level). The goal of this analysis is to provide data that can be used to tune and improve the QCD Monte-Carlo models of the "underlying event" that are used to simulate hadron-hadron collisions.

I. INTRODUCTION

In order to find "new" physics at a hadron-hadron collider it is essential to have Monte-Carlo models that simulate accurately the "ordinary" QCD hard-scattering events. To do this one must not only have a good model of the hard scattering part of the process, but also of the beam-beam remnants (BBR) and the multiple parton interactions (MPI). The "underlying event" (*i.e.* BBR plus MPI) is an unavoidable background to most collider observables and a good understanding of it will lead to more precise measurements at the Tevatron and the LHC. The goal of this analysis is to provide data that can be used to tune and improve the QCD Monte-Carlo models of the "underlying event". Fig. 1.1 illustrates the way the QCD Monte-Carlo models simulate a proton-antiproton collision in which a "hard" 2-to-2 parton scattering with transverse momentum, p_T(hard), has occurred. The resulting event contains particles that

originate from the two outgoing partons (*plus initial and final-state radiation*) and particles that come from the breakup of the proton and antiproton (*i.e.* BBR). The "beam-beam remnants" are what is left over after a parton is knocked out of each of the initial two beam hadrons. It is one of the reason hadron-hadron collisions are more "messy" than electron-positron annihilations and no one really knows how it should be modeled. For the QCD Monte-Carlo models the "beam-beam remnants" are an important component of the "underlying event". Also, it is possible that multiple parton scattering contributes to the "underlying event". Fig. 1.2 shows the way PYTHIA [1] models the "underlying event" in proton-antiproton collision by including multiple parton interactions. In addition to the hard 2-to-2 parton-parton scattering and the "beam-beam remnants", sometimes there are additional "semi-hard" 2-to-2 parton-parton scattering that contribute particles to the "underlying event". The "hard scattering" component consists of the outgoing two jets plus initial and final-state radiation.

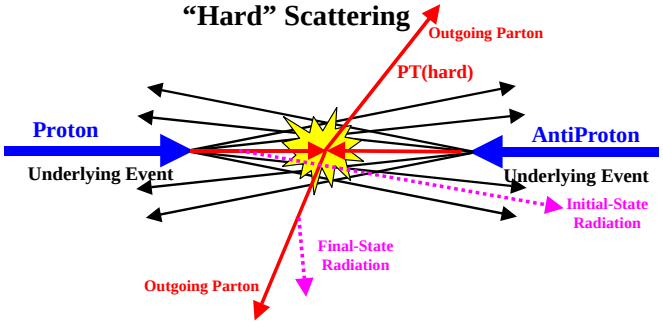

Fig. 1.1. Illustration of the way QCD Monte-Carlo models simulate a proton-antiproton collision in which a "hard" 2-to-2 parton scattering with transverse momentum, P_T(hard), has occurred. The resulting event contains particles that originate from the two outgoing partons (plus initial and final-state radiation) and particles that come from the breakup of the proton and antiproton (*i.e.* "beam-beam remnants"). The "underlying event" is everything except the two outgoing hard scattered "jets" and consists of the "beam-beam remnants" plus initial and final-state radiation. The "hard scattering" component consists of the outgoing two jets plus initial and final-state radiation.

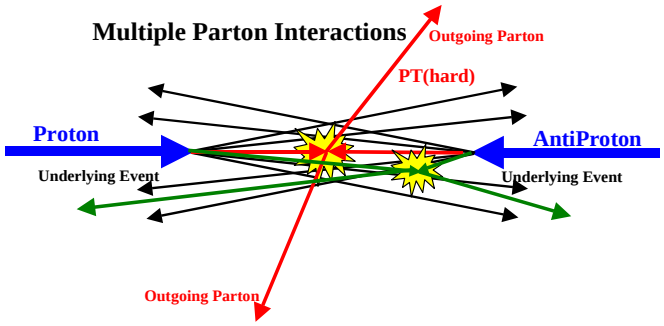

Fig. 1.2. Illustration of the way PYTHIA models the "underlying event" in proton-antiproton collision by including multiple parton interactions. In addition to the hard 2-to-2 parton-parton scattering with transverse momentum, P_T(hard), there is a second "semi-hard" 2-to-2 parton-parton scattering that contributes particles to the "underlying event".

As illustrated in Fig. 1.3, the "underlying event" consists of particles that arise from the BBR plus MPI, however, these two components cannot be uniquely separated from particles that come from the initial and final-state radiation. Hence, a study of the "underlying event" inevitably involves a study of the BBR plus MPI plus initial and final-state radiation. As shown in Fig. 1.4, Drell-Yan lepton-pair production provides an excellent place to study the "underlying event". Here one studies the outgoing charged particles (excluding the lepton pair) as a function of the lepton-pair invariant mass and as a function of the lepton-pair transverse

momentum. Unlike high p_T jet production for lepton-pair production there is no final-state gluon radiation.

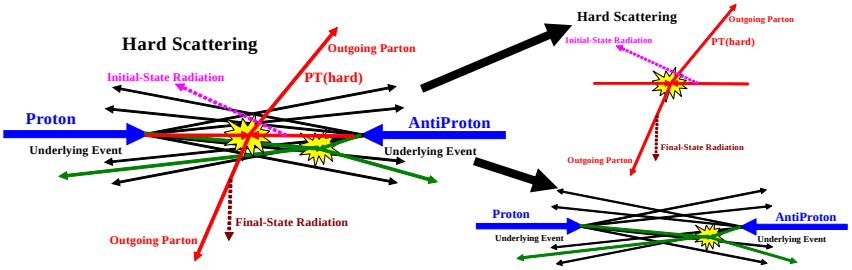

Fig. 1.3. Illustration of the way QCD Monte-Carlo models simulate a proton-antiproton collision in which a "hard" 2-to-2 parton scattering with transverse momentum, P_T(hard), has occurred. The "hard scattering" component of the event consists of particles that result from the hadronization of the two outgoing partons (*i.e.* the initial two "jets") plus the particles that arise from initial and final state radiation (*i.e.* multijets). The "underlying event" consists of particles that arise from the "beam-beam remnants" and from multiple parton interactions.

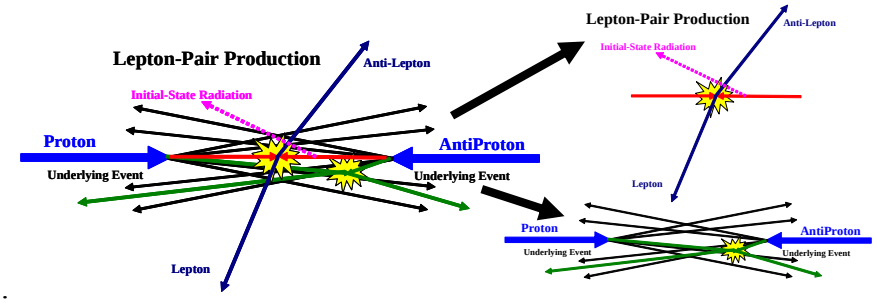

Fig. 1.4. Illustration of the way QCD Monte-Carlo models simulate Drell-Yan lepton-pair production. The "hard scattering" component of the event consists of the two outgoing leptons plus particles that result from initial-state radiation. The "underlying event" consists of particles that arise from the "beam-beam remnants" and from multiple parton interactions.

Hard scattering collider "jet" events have a distinct topology. On the average, the outgoing hadrons "remember" the underlying the 2-to-2 hard scattering subprocess. An typical hard scattering event consists of a collection (or burst) of hadrons traveling roughly in the direction of the initial two beam particles and two collections of hadrons (*i.e.* "jets") with large transverse momentum. The two large transverse momentum "jets" are roughly back to back in azimuthal angle. One can use the topological structure of hadron-hadron collisions to study the "underlying event". We use the direction of the leading jet in each event to define four regions of η-ϕ space. As illustrated in Fig. 1.5, the direction of the leading jet, jet#1, in high p_T jet production or the Z-boson in Drell-Yan production is used to define correlations in the azimuthal angle, $\Delta\phi$. The angle $\Delta\phi = \phi - \phi_{jet\#1}$ ($\Delta\phi = \phi - \phi_Z$) is the relative azimuthal angle between a charged particle and the direction of jet#1 (direction of the Z-boson). The "toward" region is defined by $|\Delta\phi| < 60^o$ and $|\eta| < 1$, while the "away" region is $|\Delta\phi| > 120^o$ and $|\eta| < 1$. The two "transverse" regions $60^o < \Delta\phi < 120^o$ and $60^o < -\Delta\phi < 120^o$ are referred to as "transverse 1" and "transverse 2". The overall "transverse" region corresponds to combining the "transverse 1" and "transverse 2" regions. In high p_T jet production, the "toward" and "away" regions receive large contributions from the to the outgoing high p_T jets, while the "transverse" region is perpendicular to the plane of the hard 2-to-2 scattering and is therefore very sensitive to the "underlying event". For Drell-Yan production both the "toward" and the "transverse" region are very

sensitive to the "underlying event", while the "away" region receives large contributions from the "away-side" jet from the 2-to-2 processes: $q + \bar{q} \to Z + g$, $q + g \to Z + q$, $\bar{q} + g \to Z + \bar{q}$.

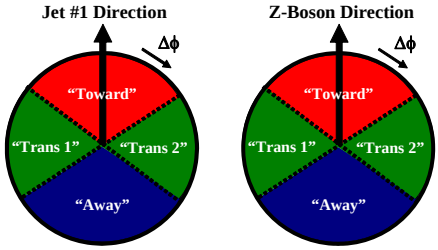

Fig. 1.5. Illustration of correlations in azimuthal angle $\Delta\phi$ relative to (*left*) the direction of the leading jet (highest p_T jet) in the event, jet#1, in high p_T jet production or (*right*) the direction of the Z-boson in Drell-Yan production. The angle $\Delta\phi = \phi - \phi_{jet\#1}$ ($\Delta\phi = \phi - \phi_Z$) is the relative azimuthal angle between charged particles and the direction of jet#1 (Z-boson). The "toward" region is defined by $|\Delta\phi| < 60^o$ and $|\eta| < 1$, while the "away" region is $|\Delta\phi| > 120^o$ and $|\eta| < 1$. The two "transverse" regions $60^o < \Delta\phi < 120^o$ and $60^o < -\Delta\phi < 120^o$ are referred to as "transverse 1" and "transverse 2". Each of the two "transverse" regions have an area in η-ϕ space of $\Delta\eta\Delta\phi = 4\pi/6$. The overall "transverse" region corresponds to combining the "transverse 1" and "transverse 2" regions.

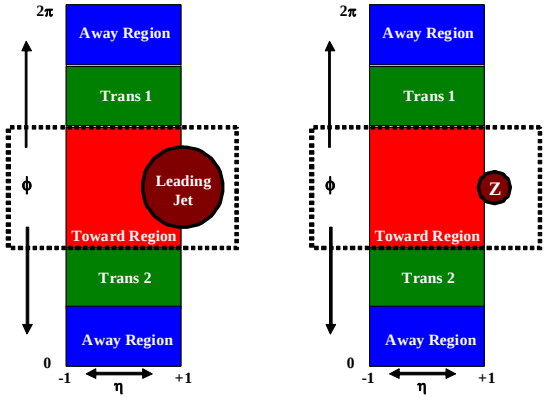

Fig. 1.6. Illustration of correlations in azimuthal angle $\Delta\phi$ relative to (*left*) the direction of the leading jet (highest p_T jet) in the event, jet#1, in high p_T jet production or (*right*) the direction of the Z-boson in Drell-Yan production. The angle $\Delta\phi = \phi - \phi_{jet\#1}$ ($\Delta\phi = \phi - \phi_Z$) is the relative azimuthal angle between charged particles and the direction of jet#1 (Z-boson). The "toward" region is defined by $|\Delta\phi| < 60^o$ and $|\eta| < 1$, while the "away" region is $|\Delta\phi| > 120^o$ and $|\eta| < 1$. The two "transverse" regions $60^o < \Delta\phi < 120^o$ and $60^o < -\Delta\phi < 120^o$ are referred to as "transverse 1" and "transverse 2". We examine charged particles in the range $p_T > 0.5$ GeV/c and $|\eta| < 1$ and $|\eta| < 1$. For high p_T jet production, we require that the leading jet in the event be in the region $|\eta(jet\#1)| < 2$ (referred to as "leading jet" events). For Drell-Yan production we require that invariant mass of the lepton-pair be in the region $81 < M(pair) < 101$ GeV/c^2 with $|\eta(pair)| < 6$ (referred to as "Z-boson" events).

As illustrated in Fig. 1.6, we study charged particles in the range $p_T > 0.5$ GeV/c and $|\eta| < 1$ in the "toward", "away" and "transverse" regions. For high p_T jet production, we require that the leading jet in the event be in the region $|\eta(jet\#1)| < 2$ (referred to as "leading jet" events). The jets are constructed using the MidPoint algorithm ($R = 0.7$, $f_{merge} = 0.75$) . For Drell-Yan production we require that invariant mass of the lepton-pair be in the region $70 < M(pair) < 110$ GeV/c^2 with $|\eta(pair)| < 6$ (referred to as "Z-boson" events).

As shown in Fig. 1.7, for both "leading jet" and "Z-boson" events we define a variety of MAX and MIN "transverse" regions ("transMAX" and "transMIN") which helps separate the "hard component" (initial and final-state radiation) from the "beam-beam remnant" component [2]. MAX (MIN) refer to the "transverse" region containing largest (smallest) number of charged particles or to the region containing the largest (smallest) scalar p_T sum of charged

particles. For events with large initial or final-state radiation the "transMAX" region would contain the third jet in high p_T jet production or the second jet in Drell-Yan production while both the "transMAX" and "transMIN" regions receive contributions from the beam-beam remnants. Thus, the "transMIN" region is very sensitive to the beam-beam remnants, while the "transMAX" minus the "transMIN" (*i.e.* "transDIF") is very sensitive to initial and final-state radiation.

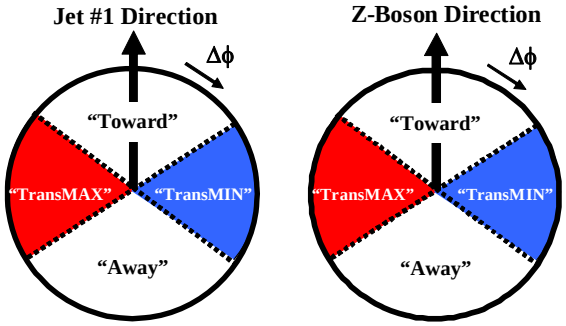

Fig. 1.7. Illustration of correlations in azimuthal angle Δϕ relative to the direction of the leading jet (highest p_T jet) in the event, jet#1 for "leading jet" events (*left*) and of correlations in azimuthal angle Δϕ relative to the direction of the Z-boson (*right*) in "Z-boson" events. The angle Δϕ is the relative azimuthal angle between charged particles and the direction of jet#1 or the Z-boson. On an event by event basis, we define "transMAX" ("transMIN") to be the maximum (minimum) of the two "transverse" regions, $60^o < \Delta\phi < 120^o$ and $60^o < -\Delta\phi < 120^o$. "TransMAX" and "transMIN" each have an area in η-ϕ space of $\Delta\eta\Delta\phi = 4\pi/6$. The overall "transverse" region includes both the "transMAX" and the "transMIN" region.

Table 1.1. Observables examined in this analysis as they are defined at the particle level and the detector level. Charged tracks are considered "good" if they pass the track selection criterion. The mean charged particle $\langle p_T \rangle$ is constructed on and event-by-event basis and then averaged over the events. For the average p_T and the PT_{max} we require that there is at least one charge particle present. The PTsum density is taken to be zero if there are no charged particles present. Particle are considered stable if $c\tau > 10$ mm (*i.e.* K_s, Λ, Σ, Ξ, and Ω are kept stable) .

Observable	Particle Level	Detector level
$dN/d\eta d\phi$	Number of stable charged particles per unit η-ϕ ($p_T > 0.5$ GeV/c, $\|\eta\| < 1$)	Number of "good" tracks per unit η-ϕ ($p_T > 0.5$ GeV/c, $\|\eta\| < 1$)
$dPT/d\eta d\phi$	Scalar p_T sum of stable charged particles per unit η-ϕ ($p_T > 0.5$ GeV/c, $\|\eta\| < 1$)	Scalar p_T sum of "good" tracks per unit η-ϕ ($p_T > 0.5$ GeV/c, $\|\eta\| < 1$)
$\langle p_T \rangle$	Average p_T of stable charged particles ($p_T > 0.5$ GeV/c, $\|\eta\| < 1$) Require at least 1 charged particle	Average p_T of "good" tracks ($p_T > 0.5$ GeV/c, $\|\eta\| < 1$) Require at least 1 "good" track
PT_{max}	Maximum p_T stable charged particle ($p_T > 0.5$ GeV/c, $\|\eta\| < 1$) Require at least 1 charged particle	Maximum p_T "good" charged tracks ($p_T > 0.5$ GeV/c, $\|\eta\| < 1$) Require at least 1 "good" track
"Jet"	MidPoint algorithm R = 0.7 f_{merge} = 0.75 applied to stable particles	MidPoint algorithm R = 0.7 f_{merge} = 0.75 applied to calorimeter cells

The data are corrected to the particle level. Table 1.1 shows the observables that are considered in this analysis as they are defined at the particle level and detector level. Since we will be studying regions in η-ϕ space with different areas, we will construct densities by dividing

by the area. For example, the number density, $dN/d\eta d\phi$, corresponds the number of charged particles per unit η-ϕ and the PT_{sum} density, $dPT/d\eta d\phi$, corresponds the amount of charged scalar p_T sum per unit η-ϕ. The corrected observables are then compared with QCD Monte-Carlo predictions at the particle level (*i.e.* generator level).

A discussion of the QCD Monte-Model tunes is presented in Section II. In Section III we discuss the data selection, track cuts, and the method we use to correct the data to the particle level. Section IV contains the results for "leading jet" and "Z-boson" events and comparisons with the QCD Monte-Carlo models. Section V is reserved for the summary and conclusions.

II. QCD Monte-Carlo Model Tunes

PYTHIA Tune A was determined by fitting the CDF Run 1 "underlying event" data [3] and, at that time, we did not consider the Z-boson data. Tune A does not fit the CDF Run 1 Z-boson p_T distribution very well [4]. PYTHIA Tune AW fits the Z-boson p_T distribution as well as the "underlying event" at the Tevatron [5]. For "leading jet" production Tune A and Tune AW are nearly identical. Table 2.1 shows the parameters for several PYTHIA 6.2 tunes. PYTHIA Tune DW is very similar to Tune AW except PARP(67) = 2.5, which is the preferred value determined by DØ in fitting their dijet $\Delta\phi$ distribution [6]. PARP(67) sets the high p_T scale for initial-state radiation in PYTHIA. It determines the maximal parton virtuality allowed in time-like showers. Tune DW and Tune DWT are identical at 1.96 TeV, but Tune DW and DWT extrapolate differently to the LHC. Tune DWT uses the ATLAS energy dependence, PARP(90) = 0.16, while Tune DW uses the Tune A value of PARP(90) = 0.25. All these tunes use CTEQ5L.

The first 9 parameters in Table 2.1 tune the multiple parton interactions (MPI). PARP(62), PARP(62), and PARP(62) tune the initial-state radiation and the last three parameters set the intrinsic k_T of the partons within the incoming proton and antiproton.

Table 2.1. Parameters for several PYTHIA 6.2 tunes. Tune A is the CDF Run 1 "underlying event" tune. Tune AW and DW are CDF Run 2 tunes which fit the existing Run 2 "underlying event" data and fit the Run 1 Z-boson p_T distribution. The ATLAS Tune is the tune used in the ATLAS TRD. Tune DWT use the ATLAS energy dependence for the MPI, PARP(90). The first 9 parameters tune the multiple parton interactions. PARP(62), PARP(62), and PARP(62) tune the initial-state radiation and the last three parameters set the intrinsic k_T of the partons within the incoming proton and antiproton.

Parameter	Tune A	Tune AW	Tune DW	Tune DWT	ATLAS
PDF	CTEQ5 L	CTEQ5 L	CTEQ5 L	CTEQ5 L	CTEQ5 L
MSTP(81)	1	1	1	1	1
MSTP(82)	4	4	4	4	4
PARP(82)	2.0	2.0	1.9	1.9409	1.8
PARP(83)	0.5	0.5	0.5	0.5	0.5
PARP(84)	0.4	0.4	0.4	0.4	0.5
PARP(85)	0.9	0.9	1.0	1.0	0.33
PARP(86)	0.95	0.95	1.0	1.0	0.66
PARP(89)	1800	1800	1800	1960	1000
PARP(90)	0.25	0.25	0.25	0.16	0.16
PARP(62)	1.0	1.25	1.25	1.25	1.0
PARP(64)	1.0	0.2	0.2	0.2	1.0
PARP(67)	4.0	4.0	2.5	2.5	1.0
MSTP(91)	1	1	1	1	1

PARP(91)	1.0	2.1	2.1	2.1	1.0
PARP(93)	5.0	15.0	15.0	15.0	5.0

Table 2.2. Shows the computed value of the multiple parton scattering cross section for the various PYTHIA 6.2 tunes.

Tune	**σ(MPI) at 1.96 TeV**	**σ(MPI) at 14 TeV**
A, AW	309.7 mb	484.0 mb
DW	351.7 mb	549.2 mb
DWT	351.7 mb	829.1 mb
ATLAS	324.5 mb	768.0 mb

Table 2.2 shows the computed value of the multiple parton scattering cross section for the various tunes. The multiple parton scattering cross section (divided by the total inelastic cross section) determines the average number of multiple parton collisions per event.

JIMMY [7] is a multiple parton interaction model which can be added to HERWIG [8] to improve agreement with the "underlying event" observables. To compare with the "Z-boson" data we have constructed a HERWIG (with JIMMY MPI) tune with JMUEO = 1, PTJIM = 3.6 GeV/c, JMRAD(73) = 1.8, and JMRAD(91) = 1.8.

II. ANALYSIS STRATEGY

(1) Data Sample and Event Selection

The CDF Run II detector, in operation since 2001, is an azimuthally and forward-backward symmetric solenoidal particle detector [9]. It combines precision charged particle tracking with fast projective calorimetry and fine grained muon detection. Tracking systems are designed to detect charged particles and measure their momenta (curvature gives the momentum and sign of charge) and displacements from the point of collision, termed the primary interaction vertex. The tracking system consists of a silicon microstrip system and an open-cell wire drift chamber, termed the Central Outer Tracker (COT) that surrounds the silicon. Segmented electromagnetic and hadronic sampling calorimeters surround the tracking system and measure the energy of interacting particles. Particles make showers which deposit energy and are sampled via their ionization. The muon system resides beyond the calorimeters. When interacting with matter, muons act as minimally ionizing particles (low bremsstrahlung radiation due to their relatively large mass); they only deposit small amounts of ionization energy in the material. They are the only particles likely to penetrate both the tracking and five absorption lengths of calorimeter steel, and leave tracks in the muon detection system.

At CDF the positive z-axis is defined to lies along the incident proton beam direction. The "leading jet" data and lepton-pair data corresponds to an integrated luminosity of about 2.2 fb^{-1} and 2.7 fb^{-1}, respectively. For both data sets we require one and only one primary vertex within the fiducial region $|Z_{vertex}| \leq 60$ cm centered around the nominal CDF z =0.

(2) Jet Selection

Jets are selected using the MidPoint cone based algorithm with a cone size of 0.7 and $f_{merge} = 0.75$. For the "leading jet" events we require that the highest p_T jet in the calorimeter ($|\eta| < 3.6$) lie in the range $|\eta| < 2$ or the event is rejected.

(3) Lepton Selection

Dielectron events are triggered online by either one central ($|\eta| < 1.1$) electron candidate with $E_T > 18$ GeV and a track with $p_T > 18$ GeV/c associated to it, or by two electromagnetic clusters with $E_T > 18$ GeV and $|\eta| < 3.2$ where no track association is required. We consider only central electrons with $E_T > 20$ GeV and $|\eta| < 1$ that also have a track matched to the calorimeter cluster. The electrons also have to pass certain quality criteria to verify that they are consistent with the electromagnetic shower characteristics as expected for electrons [10].

Dimuon events are triggered on at least one muon candidate that has a signal in one of the muon chambers with $|\eta| < 1$and $p_T > 18$ GeV/c. The second muon candidate is not required to have a signal in the muon chambers but it must have hits in the COT. We consider only muon candidates with $p_T > 20$ GeV and $|\eta| < 1$. All muon candidates are required to have calorimeter energy deposits consistent with those expected from a minimum ionizing particle. In addition, we employ a time-of-flight filter to remove cosmic ray muons.

All leptons are required to be isolated from other particles in the event by a distance of $R = \sqrt{(\Delta\eta)^2 + (\Delta\phi)^2} < 0.4$.

(4) Lepton-Pair Selection

The lepton pairs are formed by oppositely charged leptons, with the requirement that the z positions of the two leptons satisfy $|\Delta z| < 4$ cm, to ensure that both leptons came from the same primary collision. For the "Z-boson" data we require that both leptons have $p_T > 20$ GeV/c and $|\eta| < 1$ and that the invariant mass of the lepton-pair be in the range $70 < M(pair) < 110$ GeV, with $|\eta(pair)| < 6$. Studies have shown that the lepton-pair backgrounds (mostly from QCD jets and W+jets) are negligible in the region of the Z-boson [11].

(5) Track Selection

We consider charged tracks that have been measured by the central outer tracker (COT). The COT [12] is a cylindrical open-cell 17 drift chamber with 96 sense wire layers grouped into eight alternating superlayers of stereo 18 and axial wires. Its active volume covers $40 < r < 137$ cm and $|z| < 155$ cm, thus providing fiducial coverage in $|\eta| \leq 1.1$ to tracks originating within $|z| \leq 60$ cm. We include tracks in the region $0.5 < p_T < 150$ GeV/c and $|\eta| < 1$ where COT efficiency is high. The upper limit of 150 GeV/c is chosen to prevent miss-measured tracks with very high p_T from contributing since at very high p_T the track resolution deteriorates. The tracks are required to hit at least two axial segments with more than 10 total hits and at least two stereo segments with more than 10 total hits in COT. In addition, the tracks are required to point back to the primary vertex. We consider two track selections; "loose" and "tight". The "loose" track selection requires $|d_0| < 1.0$ cm and $|z - Z_{vtx}| < 3$ cm, where d_0 is the beam corrected transverse impact parameter and $z - Z_{vtx}$ is the distance on the z-axis (*i.e.* beam axis) between the track from the primary vertex. The "tight" track selection requires that $|d_0| < 0.5$ cm and $|z - Z_{vtx}| < 2$ cm. The "loose" criterion is similar to the Run 1 "underlying event" analysis [3].

(6) Correcting to the Particle Level and Systematic Uncertainties

The raw data at the detector level must be corrected to the particle level. The particle level corresponds to the true event before detector effects. We rely on the QCD Monte-Carlo models and the CDF detector simulation (CDFSIM) to correct the measured tracks back to the charged particle level (*i.e.* generator level). The generator level charged particles have $p_T > 0.5$ GeV/c, $|\eta| < 1$, and are kept stable if $c\tau > 10$ mm. Hence, to compare the corrected data with QCD Monte-Carlo model predictions one must keep the K_{short} meson stable as well as the following baryons; Λ, Σ, Ξ, and Ω.

For "leading jet" events the QCD Monte-Carlo model is used to calculate the observables in Table 1.1 at the particle level (*i.e.* generator level) in bins of particle jet#1 p_T (GEN) and at the detector level in bins of calorimeter jet#1 p_T (CDFSIM). The detector level data in bins of calorimeter jet#1 p_T are corrected by multiplying by the QCD Monte-Carlo "correction" factor, GEN/CDFSIM. This is done bin-by-bin for every observable. We refer to the ratio CDFSIM/GEN as the "response" factor for that observable with the "correction" factor being the reciprocal. Smooth curves are drawn through the QCD Monte-Carlo predictions at both the generator level (GEN) and the detector level (CDFSIM) to aid in comparing the theory with the data and also to construct the "correction" factors. This one step correction method simultaneously corrects for mismeasurement of the leading jet transverse momentum (*i.e.* jet energy scale) and for missed and/or fake tracks.

The correction factors are different for every observable and they are different for the "tight" and "loose" track selection criterion. The "tight" track criterion results in less tracks than the "loose" criterion and hence the Monte-Carlo corrections factors are different. If the Monte-Carlo described the data perfectly and if CDFSIM was exact than the corrected observable would be identical regardless of the track selection criterion. Using PYTHIA Tune A for the "leading jet" events and PYTHIA Tune AW for the "Z-boson" events we find that the "loose" and "tight" track selections do result in nearly the same particle level result for all the observables presented in this analysis. The differences are used as a source of systematic error and are added in quadrature to the statistical errors.

The corrections factors are typically small (less that 5%) except in regions where the charged particle density becomes large which occurs in the "toward" and "away" regions for "leading jet" production. The efficiency of detecting charged tracks decreases when the density of tracks becomes large. For the "leading jet" events we have also used HERWIG (without MPI) instead of PYTHIA Tune A to correct the data to the particle level. We use the differences in the corrected data as an addition source of systematic error (added in quadrature).

An important systematic error arises from the uncertainty in the jet energy scale, P_T(jet#1). The CDF detector simulation does not reproduce perfectly the response of the calorimeter. The overall systematic uncertainty in the CDF jet energy scale (JES) is a function of the jet p_T [13]. The uncertainty is about 3% at high p_T and increases to around 8% at low p_T. After correcting the data to the particle level we shift P_T(jet#1) up and down by this additional uncertainty with the bin-by-bin differences in the observables in Table 1.1 used as another systematic error (added in quadrature). The JES systematic errors are large in the "toward" and "away" region where the observables are varying rapidly with P_T(jet#1).

We investigated the dependence of the corrected data to our upper limit of $PT_{max}(cut)$ = 150 GeV/c which was applied to all tracks. The sensitivity of the results to this choice of upper limit was checked by changing the upper limit to $PT_{max}(cut) = 1.5 \times ET_{max}(tower)$. Here one looks, on an event-by-event bases, at all the towers in the region $|\eta| < 1$ and sets the maximum p_T track cut to be equal to 1.5 times the E_T of the tower with the largest transverse energy. High pT mismeasured tracks do not deposit energy in the calorimeter. The two track cuts produce slightly different correction factors, however, after correcting to the particle level the results are nearly identical. For the "leading jet" analysis the differences were used as an additional systematic error (added in quadrature).

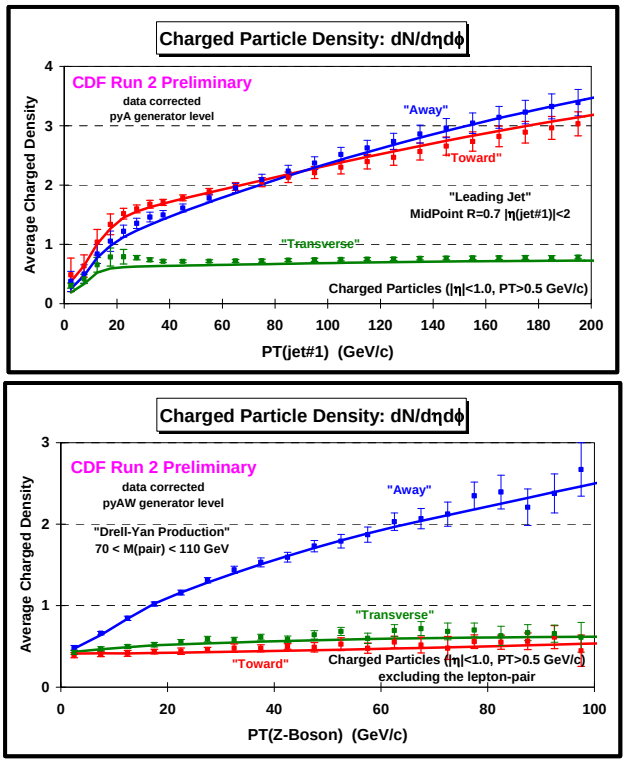

Fig. 3.1. CDF data at 1.96 TeV on the density of charged particles, $dN/d\eta d\phi$, with $p_T > 0.5$ GeV/c and $|\eta| < 1$ for "leading jet" (*top*) and "Z-boson" (*bottom*) events as a function of the leading jet p_T and $p_T(Z)$, respectively, for the "toward", "away", and "transverse" regions. The data are corrected to the particle level and are compared with PYTHIA Tune A and Tune AW, respectively, at the particle level (*i.e.* generator level).

Although we require one and only one high quality 12 vertex, the observables in Table 1.1 can still be affected by pile-up (*i.e.* more that one proton-antiproton collision in the event). Tracks are required to point back to the primary vertex, but the track observables are affected by pile-up when two vertices overlap. Vertices within about 3 cm of each other merge together as one. In the "leading jet" analysis we examined the effects of pile-up by plotting the "transverse" charged particle density and the charged PTsum density versus the instantaneous luminosity (with one and only one vertex). As the instantaneous luminosity increases so does the amount of pile-up. We found that these observables did increase slightly with increasing luminosity (roughly linearly). The "leading jet" observables in the "transverse" region are corrected for pile-up by extrapolating to the low luminosity limit. To correct the data, we define a low region, $iLumi < 25 \times 10^{30}$ $cm^{-2}s^{-1}$ (low), and a high region $iLumi > 25 \times 10^{30}$ $cm^{-2}s^{-1}$ (high), where iLumi is the instantaneous luminosity. On a bin-by-bin basis, the ratio high/low and all/low was

constructed, where all = high + low. The ratio high/low was found to be small (usually less than 1%) and could simply have been absorbed into the overall systematic errors. However, for in the "leading jet" analysis we corrected the data for pile-up by drawing a smooth curve through the ratio all/low and then dividing the data by this ratio. The size of the pile-up correction was then taken as the systematic error in making the correction and added in quadrature with the other systematic errors. For the Z-boson analysis, the pile-up corrections were less than 1% and were absorbed into the overall systematic errors.

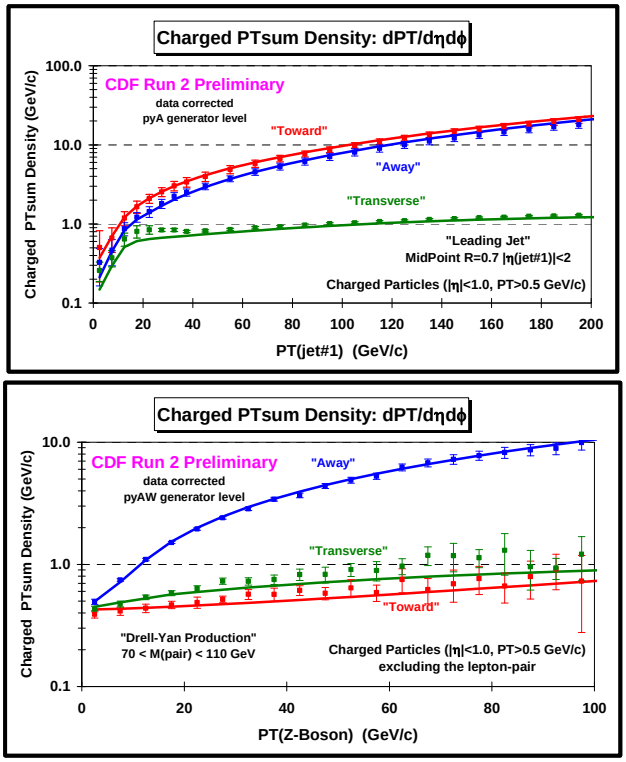

Fig. 3.2. CDF data at 1.96 TeV on the *scalar* PTsum density of charged particles, dPT/dηdϕ, with $p_T > 0.5$ GeV/c and $|\eta| < 1$ and "leading jet" (*top*) and "Z-Boson" (*bottom*) events as a function of the leading jet p_T and $p_T(Z)$, respectively, for the "toward", "away", and "transverse" regions. The data are corrected to the particle level and are compared with PYTHIA Tune A and Tune AW, respectively, at the particle level (*i.e.* generator level).

IV. RESULTS

(1) "Leading Jet" and "Z-Boson" Topologies

Fig. 3.1 and Fig. 3.2 show the data on the density of charged particles and the *scalar* PTsum density, respectively, for the "toward", "away", and "transverse" regions for "leading jet" and "Z-boson" events. For "leading jet" events the densities are plotted as a function of the leading jet p_T and for "Z-boson" events there are plotted versus $p_T(Z)$. The data are corrected to the particle level and are compared with PYTHIA Tune A ("leading jet") and Tune AW ("Z-boson") at the particle level (*i.e.* generator level). For "leading jet" events at high p_T(jet#1) the densities in the "toward" and "away" regions are much larger than in the "transverse" region because of the "toward-side" and "away-side" jets. At small p_T(jet#1) the "toward", "away", and "transverse" densities become equal and go to zero as p_T(jet#1) goes to zero. If the leading jet

has no transverse momentum then there are no charged particles. There are a lot of low transverse momentum jets and for p_T(jet#1) < 30 GeV/c and the leading jet is not always the jet resulting from the hard 2-to-2 scattering. This produces is a "bump" in the "transverse" density in the range where the "toward", "away", and "transverse" densities become similar in size. For "Z-boson" events the "toward" and "transverse" densities are both small and almost equal. The "away" density is large due to the "away-side" jet. The "toward", "away", and "transverse" densities become equal as $p_T(Z)$ goes to zero, but unlike the "leading jet" case the densities do not vanish at $p_T(Z) = 0$.

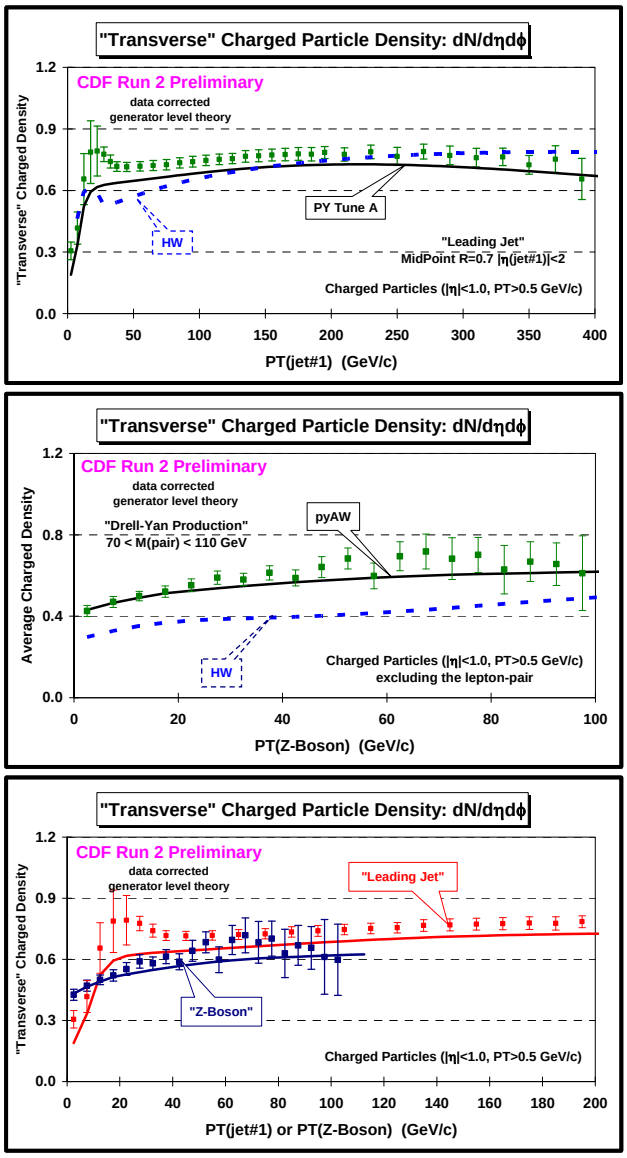

Fig. 3.3. (*top*) Data corrected to the particle level at 1.96 TeV on the density of charged particles, $dN/d\eta d\phi$, with $p_T > 0.5$ GeV/c and $|\eta| < 1$ for "leading jet" events as a function of the leading jet p_T in the "transverse" region compared with HERWIG (without MPI) and PYTHIA Tune A at the particle level (*i.e.* generator level). (*middle*) Data corrected to the particle level at 1.96 TeV on the density of charged particles, $dN/d\eta d\phi$, with $p_T > 0.5$ GeV/c and $|\eta| < 1$ for "Z-boson" events as a function of the leading jet $p_T(Z)$ in the "transverse" region compared with HERWIG (without MPI) and PYTHIA Tune AW at the particle level (*i.e.* generator level). (*bottom*) Data on the density of charged particles for "leading jet" and "Z-boson" events as a function of the leading jet p_T and $p_T(Z)$, respectively, for the "transverse" region compared with PYTHIA Tune A ("leading jet") and Tune AW ("Z-boson").

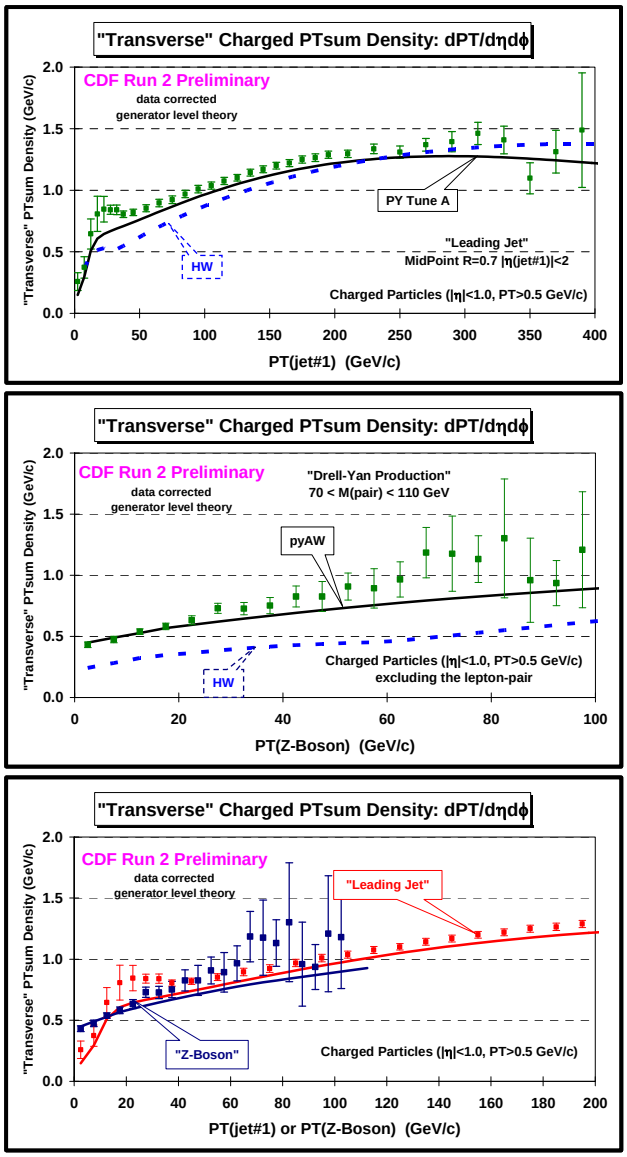

Fig. 3.4. (*top*) Data corrected to the particle level at 1.96 TeV on the *scalar* PTsum density of charged particles, dPT/dηdϕ, with $p_T > 0.5$ GeV/c and $|\eta| < 1$ for "leading jet" events as a function of the leading jet p_T in the "transverse" region compared with HERWIG (without MPI) and PYTHIA Tune A at the particle level (*i.e.* generator level). (*middle*) Data corrected to the particle level at 1.96 TeV on the *scalar* PTsum density of charged particles, dPT/dηdϕ, with $p_T > 0.5$ GeV/c and $|\eta| < 1$ for "Z-boson" events as a function of the leading jet $p_T(Z)$ in the "transverse" region compared with HERWIG (without MPI) and PYTHIA Tune AW at the particle level (*i.e.* generator level). (*bottom*) Data on the *scalar* PTsum density of charged particles for "leading jet" and "Z-boson" events as a function of the leading jet p_T and $p_T(Z)$, respectively, for the "transverse" region compared with PYTHIA Tune A ("leading jet") and Tune AW ("Z-boson").

Fig. 3.3 and Fig. 3.4 compare the data for "leading jet" events with the data for "Z-boson" events for the density of charged particles and the *scalar* PTsum density, respectively, in the "transverse" region. The data are corrected to the particle level and are compared with PYTHIA Tune A ("leading jet") , Tune AW ("Z-boson"), and HERWIG (without MPI). For large p_T(jet#1) the "transverse" densities are similar for "leading jet" and "Z-boson" events as one would expect. HERWIG (without MPI) does not produce enough activity in the "transverse" region for either process. HERWIG (without MPI) disagrees more with the "transverse" region of "Z-boson" events than it does with the "leading jet" events. This is

because there is no final-state radiation in "Z-boson" production so that the lack of MPI becomes more evident.

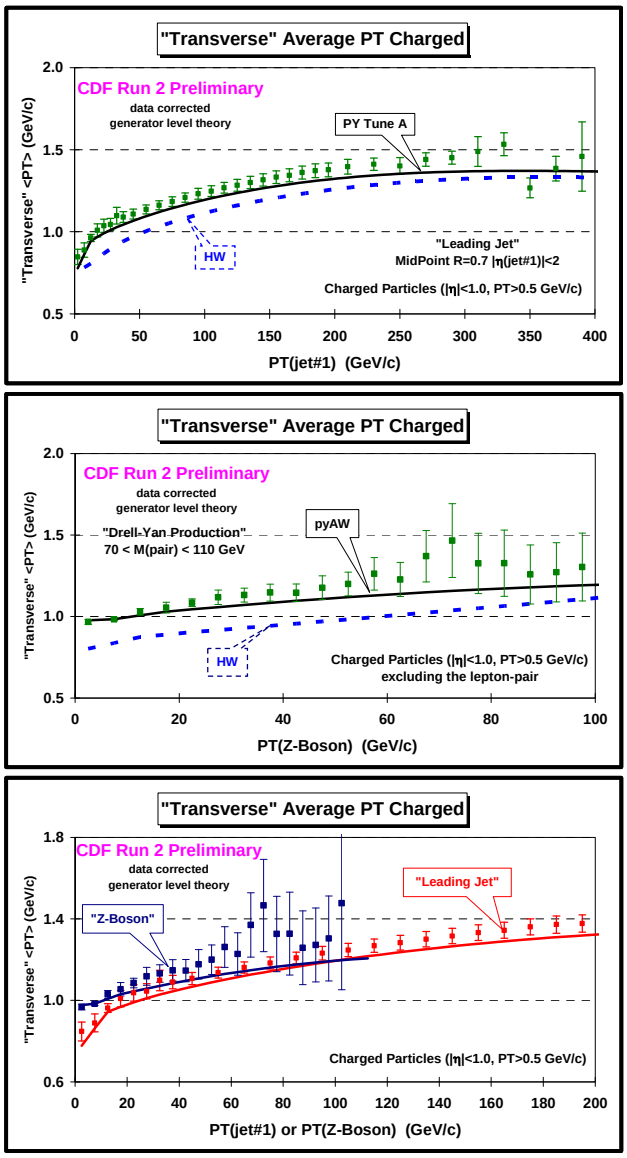

Fig. 3.5. (*top*) Data corrected to the particle level at 1.96 TeV on the average charged particle transverse momentum, $\langle p_T \rangle$, with $p_T > 0.5$ GeV/c and $|\eta| < 1$ for "leading jet" events as a function of the leading jet p_T in the "transverse" region compared with HERWIG (without MPI) and PYTHIA Tune A at the particle level (*i.e.* generator level). (*middle*) Data corrected to the particle level at 1.96 TeV on the average charged particle transverse momentum, $\langle p_T \rangle$, with $p_T > 0.5$ GeV/c and $|\eta| < 1$ for "Z-boson" events as a function of the leading jet $p_T(Z)$ in the "transverse" region compared with HERWIG (without MPI) and PYTHIA Tune AW at the particle level (*i.e.* generator level). (*bottom*) Data on the average charged particle transverse momentum for "leading jet" and "Z-boson" events as a function of the leading jet p_T and $p_T(Z)$, respectively, for the "transverse" region compared with PYTHIA Tune A ("leading jet") and Tune AW ("Z-boson").

Fig. 3.5 and Fig. 3.6 compare the data for "leading jet" events with the data for "Z-boson" events for the average charged particle p_T and the average maximum charged particle p_T, respectively, in the "transverse" region. The data are corrected to the particle level and are compared with PYTHIA Tune A ("leading jet") , Tune AW ("Z-boson"), and HERWIG (without

MPI). For HERWIG (without MPI) the p_T distributions in the "transverse" region for both processes are too "soft", resulting in an average p_T and average PT_{max} that are too small.

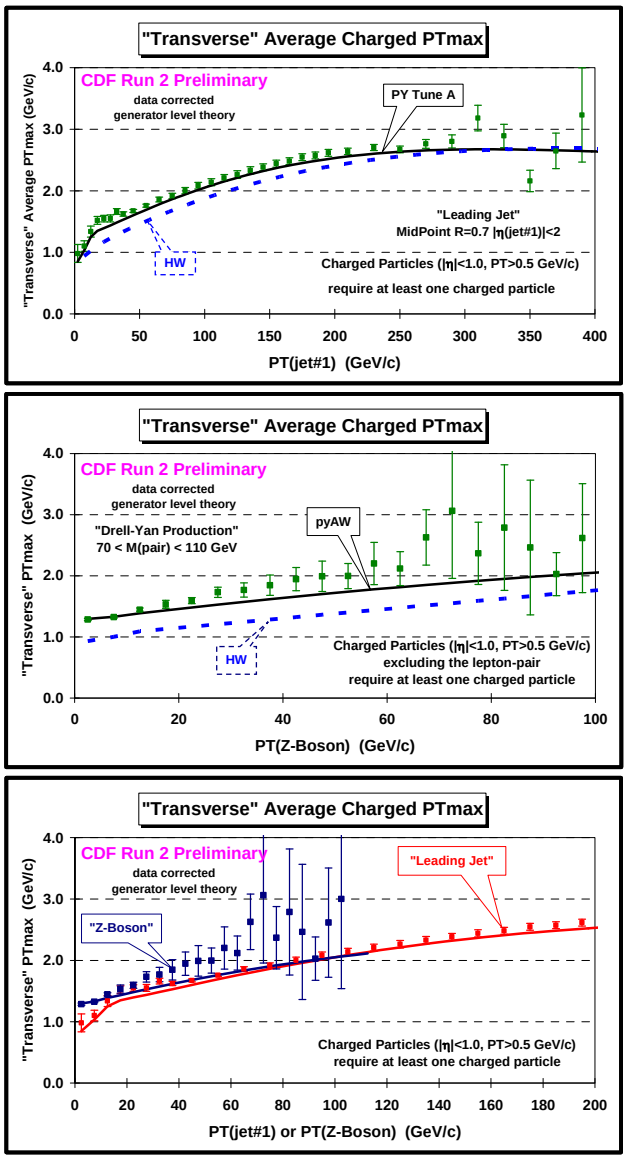

Fig. 3.6. (*top*) Data corrected to the particle level at 1.96 TeV on the average maximum charged particle transverse momentum, <PTmax>, with $p_T > 0.5$ GeV/c and $|\eta| < 1$ (require at least one charged particle) for "leading jet" events as a function of the leading jet p_T for the "transverse" region compared with HERWIG (without MPI) and PYTHIA Tune A at the particle level (*i.e.* generator level). (*middle*) Data corrected to the particle level at 1.96 TeV on the average maximum charged particle transverse momentum, <PTmax>, with $p_T > 0.5$ GeV/c and $|\eta| < 1$ (require at least one charged particle) for "Z-boson" events as a function of the leading jet $p_T(Z)$ for the "transverse" region compared with HERWIG (without MPI) and PYTHIA Tune AW at the particle level (*i.e.* generator level). (*bottom*) Data on the average maximum charged particle transverse momentum for "leading jet" and "Z-boson" events as a function of the leading jet p_T and $p_T(Z)$, respectively, for the "transverse" region compared with PYTHIA Tune A ("leading jet") and Tune AW ("Z-boson").

Fig. 3.7 and Fig. 3.8 compare the data for "leading jet" events with the data for "Z-boson" events for the density of charged particles and the *scalar* PTsum density, respectively, for the "transMAX" and "transMIN" regions. The data are corrected to the particle level and are compared with PYTHIA Tune A ("leading jet") , Tune AW ("Z-boson"), and HERWIG (without MPI).

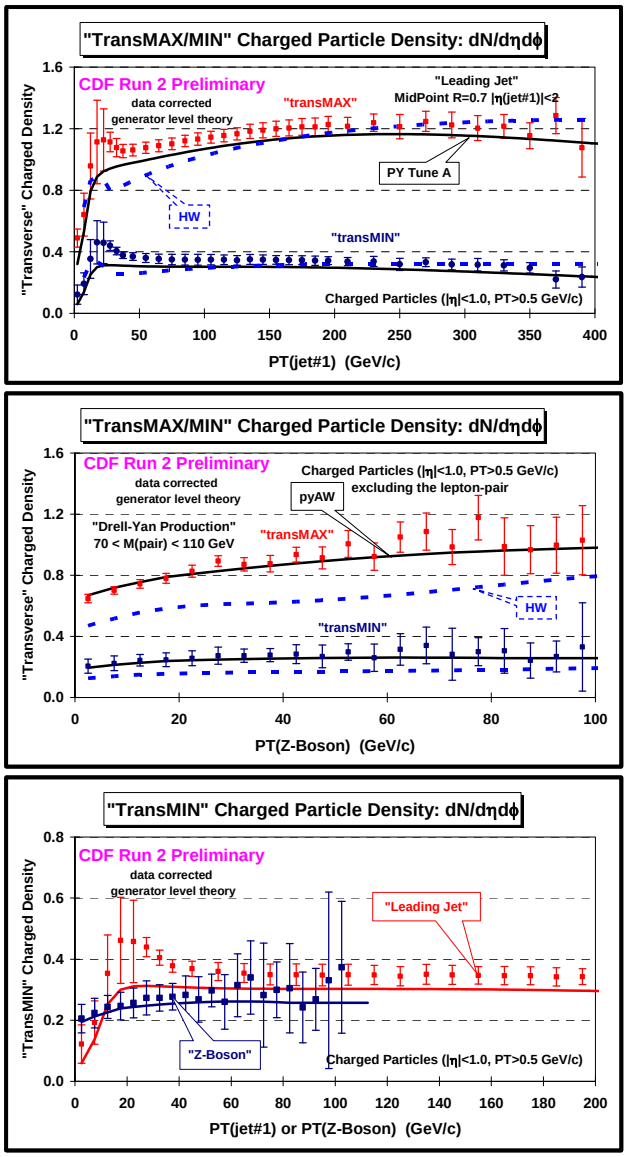

Fig. 3.7. (*top*) Data corrected to the particle level at 1.96 TeV on the density of charged particles, dN/dηdϕ, with $p_T > 0.5$ GeV/c and $|\eta| < 1$ for "leading jet" events as a function of the leading jet p_T for the "transMAX" and "transMIN" regions compared with HERWIG (without MPI) and PYTHIA Tune A at the particle level (*i.e.* generator level). (*middle*) Data corrected to the particle level at 1.96 TeV on the density of charged particles, dN/dηdϕ, with $p_T > 0.5$ GeV/c and $|\eta| < 1$ for "Z-boson" events as a function of the leading jet $p_T(Z)$ for the "transMAX" and "transMIN" regions compared with HERWIG (without MPI) and PYTHIA Tune AW at the particle level (*i.e.* generator level). (*bottom*) Data on the density of charged particles for "leading jet" and "Z-boson" events as a function of the leading jet p_T and $p_T(Z)$, respectively, for the "transMIN" region compared with PYTHIA Tune A ("leading jet") and Tune AW ("Z-boson").

Fig. 3.9 compares the data for "leading jet" events with the data for "Z-boson" events for the density of charged particles and the *scalar* PTsum density for "transDIF" = "transMAX" - "transMIN". The data are corrected to the particle level and are compared with PYTHIA Tune A ("leading jet") and Tune AW ("Z-boson"). The "transDIF" region is sensitive to the hard initial-state radiation and is predicted to be very similar in the two processes.

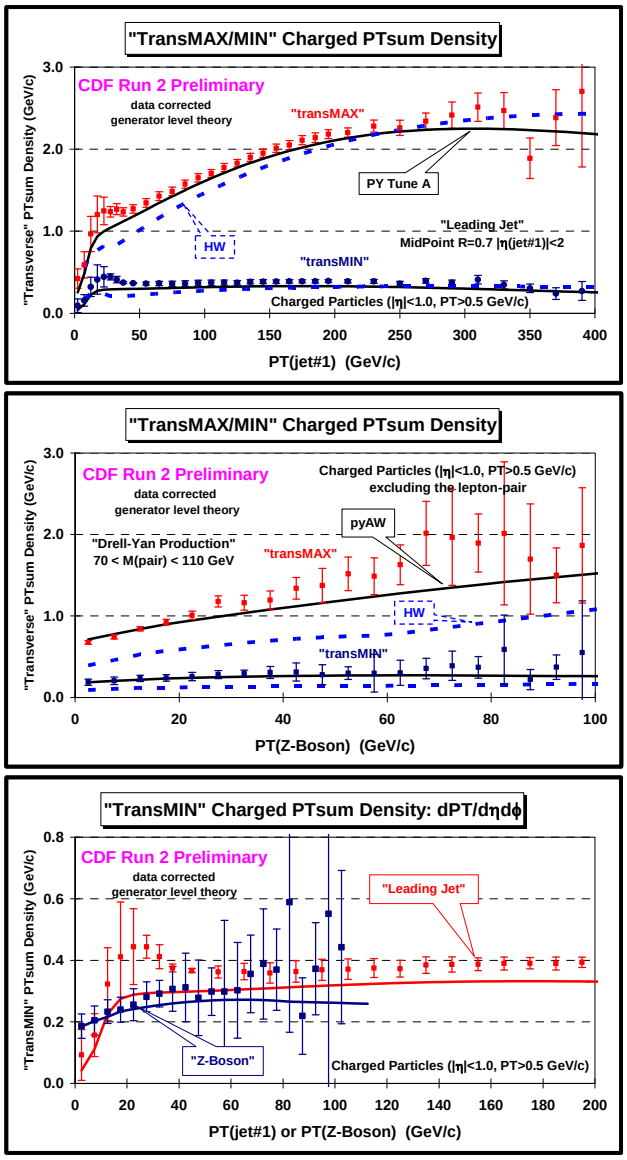

Fig. 3.8. (*top*) Data corrected to the particle level at 1.96 TeV on the *scalar* PTsum density of charged particles, dPT/dηdϕ, with $p_T > 0.5$ GeV/c and $|\eta| < 1$ for "leading jet" events as a function of the leading jet p_T for the "transMAX" and "transMIN" regions compared with HERWIG (without MPI) and PYTHIA Tune A at the particle level (*i.e.* generator level). (*middle*) Data corrected to the particle level at 1.96 TeV on the *scalar* PTsum density of charged particles, dPT/dηdϕ, with $p_T > 0.5$ GeV/c and $|\eta| < 1$ for "Z-boson" events as a function of the leading jet $p_T(Z)$ for the "transMAX" and "transMIN" regions compared with HERWIG (without MPI) and PYTHIA Tune AW at the particle level (*i.e.* generator level). (*bottom*) Data on the *scalar* PTsum density of charged particles for "leading jet" and "Z-boson" events as a function of the leading jet p_T and $p_T(Z)$, respectively, for the "transMIN" region compared with PYTHIA Tune A ("leading jet") and Tune AW ("Z-boson").

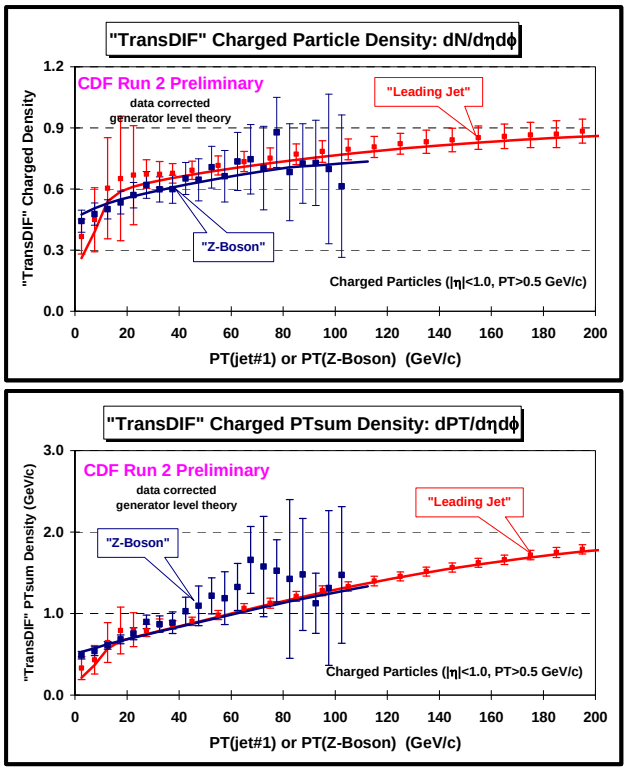

Fig. 3.9. Data at 1.96 TeV on the density of charged particles, dN/dηdϕ, with $p_T > 0.5$ GeV/c and $|\eta| < 1$ (*top*) and the *scalar* PTsum density of charged particles, dPT/dηdϕ, with $p_T > 0.5$ GeV/c and $|\eta| < 1$ (*bottom*) for "leading jet" and "Z-boson" events as a function of the leading jet p_T and $p_T(Z)$, respectively, for the "transDIF" region (transDIF = transMAX – transMIN). The data are corrected to the particle level and are compared with PYTHIA Tune A ("leading jet") and Tune AW ("Z-boson") at the particle level (*i.e.* generator level).

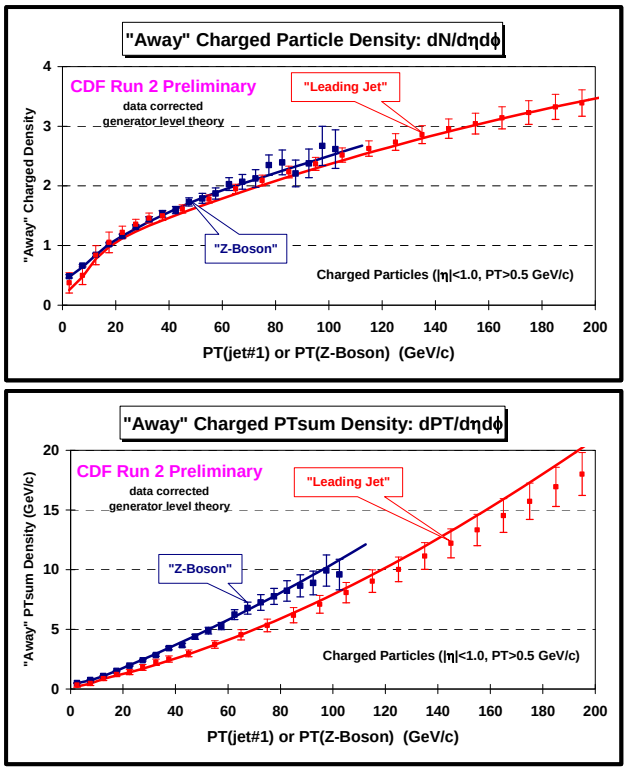

Fig. 3.10. Data at 1.96 TeV on the density of charged particles, $dN/d\eta d\phi$, with $p_T > 0.5$ GeV/c and $|\eta| < 1$ (*top*) and the *scalar* PTsum density of charged particles, $dPT/d\eta d\phi$, with $p_T > 0.5$ GeV/c and $|\eta| < 1$ (*bottom*) for "leading jet" and "Z-boson" events as a function of the leading jet p_T and $p_T(Z)$, respectively, in the "away" region. The data are corrected to the particle level and are compared with PYTHIA Tune A ("leading jet") and Tune AW ("Z-boson") at the particle level (*i.e.* generator level).

Fig. 3.10 compares the data for "leading jet" events with the data for "Z-boson" events for the density of charged particles and the *scalar* PTsum density in the "away" region. Here we do not expect the "leading jet" and "Z-boson" data to necessarily agree and it does not. However, PYTHIA Tune A and Tune AW describe the data fairly well.

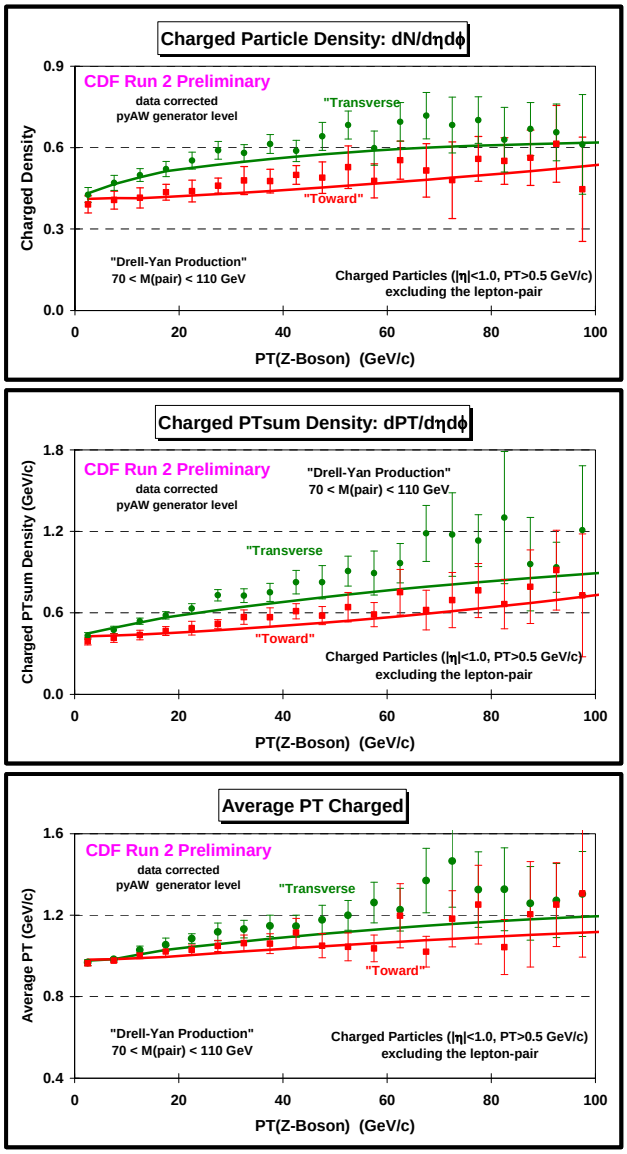

Fig. 3.11. Data at 1.96 TeV on the density of charged particles, $dN/d\eta d\phi$, with $p_T > 0.5$ GeV/c and $|\eta| < 1$ (*top*) and the *scalar* PTsum density of charged particles, $dPT/d\eta d\phi$, with $p_T > 0.5$ GeV/c and $|\eta| < 1$ (*middle*) and the average charged particle transverse momentum, $\langle p_T \rangle$, with $p_T > 0.5$ GeV/c and $|\eta| < 1$ (*bottom*) for "Z-boson" events as a function of $p_T(Z)$, in the "toward" and "transverse" regions. The data are corrected to the particle level and are compared with Tune AW at the particle level (*i.e.* generator level).

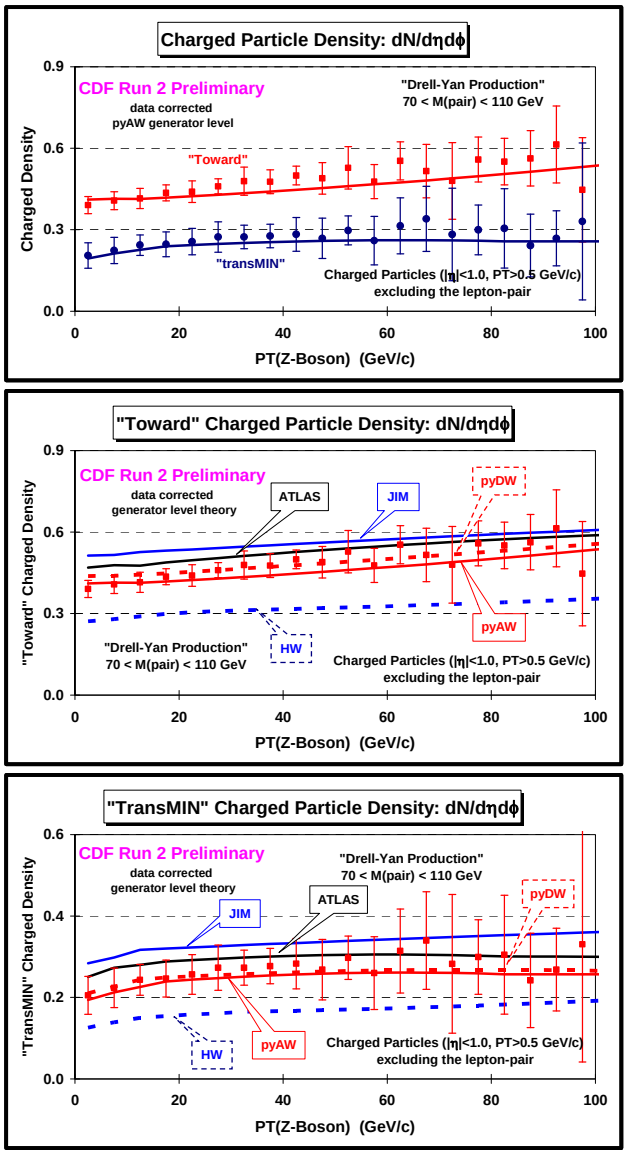

Fig. 3.12. Data corrected to the particle level at 1.96 TeV on the density of charged particles, dN/dηdϕ, with $p_T > 0.5$ GeV/c and $|\eta| < 1$ for "Z-boson" events as a function of $p_T(Z)$, in the "toward" and "transMIN" regions. (*top*) Data in the "toward" and "transMIN" regions are compared with PYTHIA Tune AW. (*middle*) Data in the "toward" region are compared with HERWIG (without MPI), HERWIG (with JIMMY MPI), and three PYTHIA MPI tunes (AW, DW, ATLAS). (*middle*) Data for the "transMIN" region are compared with HERWIG (without MPI), HERWIG (with JIMMY MPI), and three PYTHIA MPI tunes (AW, DW, ATLAS).

(2) The "Underlying Event" in Drell-Yan Production

Fig. 3.11 compares the data in the "toward" region with the data in the "transverse" region for "Z-boson" events for the density of charged particles, the *scalar* PTsum density, and the average charged particle p_T. The data are corrected to the particle level and are compared with PYTHIA Tune AW at the particle level (*i.e.* generator level). For high transverse momentum Z-boson production, particles from initial-state radiation are more likely to populate the "transverse" region than the "toward" region and hence the densities are slightly larger in the "transverse" region. PYTHIA Tune AW describes this very nicely.

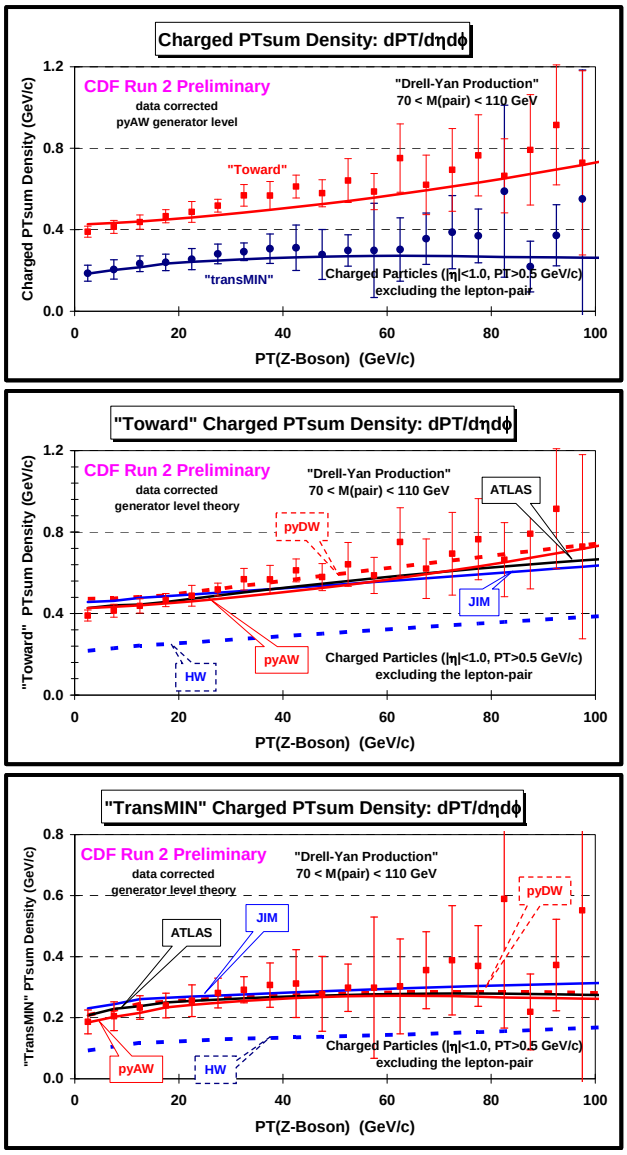

Fig. 3.13. Data corrected to the particle level at 1.96 TeV on the *scalar* charged particle PTsum density, dPT/dηdϕ, with $p_T > 0.5$ GeV/c and $|\eta| < 1$ for "Z-boson" events as a function of $p_T(Z)$, in the "toward" and "transMIN" regions. (*top*) Data for the "toward" and "transMIN" regions are compared with PYTHIA Tune AW. (*middle*) Data for the "toward" region are compared with HERWIG (without MPI), HERWIG (with JIMMY MPI), and three PYTHIA MPI tunes (AW, DW, ATLAS). (*middle*) Data for the "transMIN" region are compared with HERWIG (without MPI), HERWIG (with JIMMY MPI), and three PYTHIA MPI tunes (AW, DW, ATLAS).

The most sensitive regions to the "underlying event" in Drell-Yan production are the "toward" and the "transMIN" regions, since these regions are less likely to receive contributions from initial-state radiation. Fig. 3.12 and Fig. 3.13 shows the data for "Z-boson" events for the density of charged particles and the *scalar* PTsum density, respectively, in the "toward" and "transMIN" regions. The data are corrected to the particle level and are compared with PYTHIA Tune AW, Tune DW, the PYTHIA ATLAS tune. HERWIG (without MPI), and HERWIG (with JIMMY MPI). The densities are smaller in the "transMIN" region than in the "toward" region and this is described well by PYTHIA Tune AW. Comparing HERWIG (without MPI) with HERWIG (with JIMMY MPI) clearly shows the importance of MPI in these regions. Tune

AW and Tune DW are very similar. The ATLAS tune and HERWIG (with JIMMY MPI) agree with Tune AW for the *scalar* PTsum density in the "toward" and "transMIN" regions. However, both the ATLAS tune and HERWIG (with JIMMY MPI) produce too much charged particle density in these regions. The ATLAS tune and HERWIG (with JIMMY MPI) fit the PTsum density, but they do so by producing too many charged particles (i.e. they both have to "soft" of a p_T spectrum in these regions). This can be seen clearly in Fig. 3.14 which shows the data for "Z-boson" events on the average charged particle p_T and the average maximum charged particle p_T, in the "toward" region compared with the QCD Monte-Carlo models.

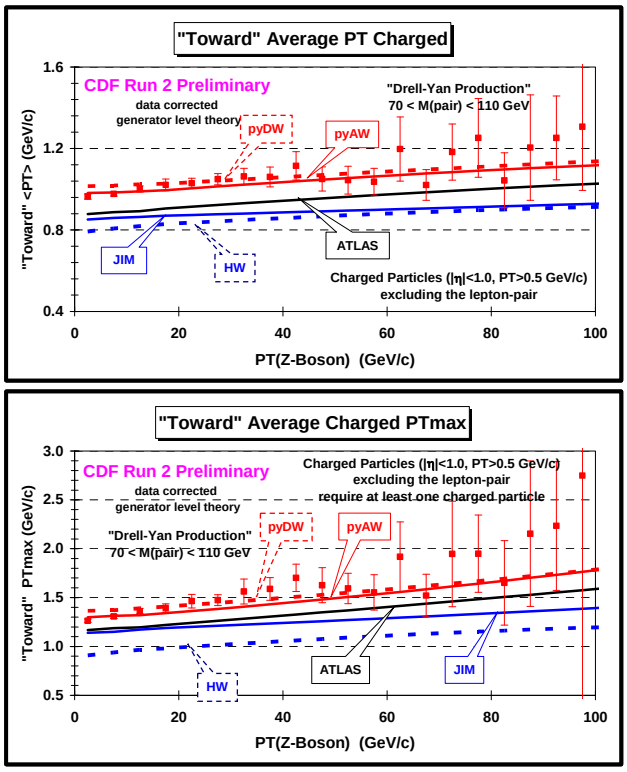

Fig. 3.14. Data corrected to the particle level at 1.96 TeV on the charged particle average transverse momentum, $\langle p_T \rangle$, with $p_T > 0.5$ GeV/c and $|\eta| < 1$ (*top*) and average maximum charged particle transverse momentum, <PTmax>, with $p_T > 0.5$ GeV/c and $|\eta| < 1$ (require at least one charged particle) (*bottom*) for "Z-boson" events as a function of $p_T(Z)$, in the "toward" region compared with HERWIG (without MPI), HERWIG (with JIMMY MPI), and three PYTHIA MPI tunes (AW, DW, ATLAS).

(3) Extrapolating Drell-Yan Production to the LHC

Fig. 3-15 shows the extrapolation of PYTHIA Tune DWT and HERWIG (without MPI) for the density of charged particles and the average transverse momentum of charged particles in the "towards" region of "Z-boson" production to 10 TeV (LHC10) and to 14 TeV (LHC14). For HERWIG (without MPI) the "toward" region of "Z-boson" production does not change much in going from the Tevatron to the LHC. Models with multiple-parton interactions like PYTHIA Tune DWT predict that the "underlying event" will become much more active (with larger $\langle p_T \rangle$) at the LHC.

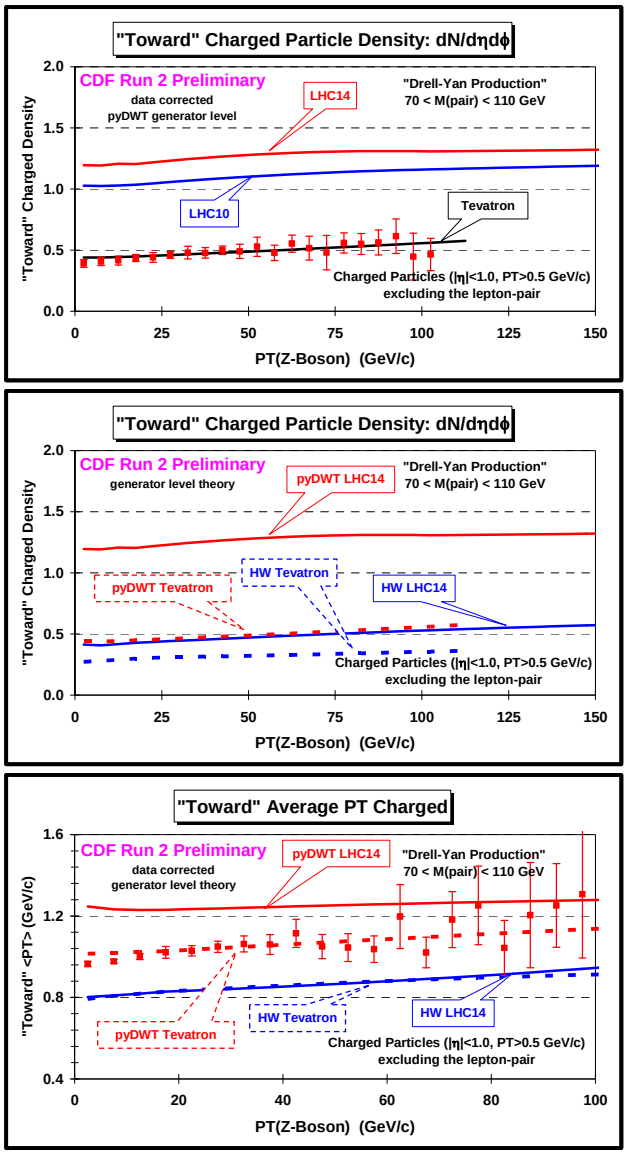

Fig. 3.15. (*top*) Data corrected to the particle level at 1.96 TeV on the density of charged particles, dN/dηdϕ, with $p_T > 0.5$ GeV/c and $|\eta| < 1$ for "Z-boson" events as a function of $p_T(Z)$, in the "toward" region compared with PYTHIA Tune DWT at 1.96 TeV (Tevatron), 10 TeV (LHC10), and 14 TeV (LHC14). (*middle*) Predictions of HERWIG (without MPI) and PYTHIA Tune DWT for the density of charged particles, dN/dηdϕ, with $p_T > 0.5$ GeV/c and $|\eta| < 1$ for "Z-boson" events as a function of $p_T(Z)$, in the "toward" region at 1.96 TeV (Tevatron) and 14 TeV (LHC14). (*bottom*) Data corrected to the particle level at 1.96 TeV on the average charged particle transverse momentum. $<p_T>$, with $p_T > 0.5$ GeV/c and $|\eta| < 1$ for "Z-boson" events as a function of $p_T(Z)$, for the "toward" region compared with HERWIG (without MPI) and PYTHIA Tune DWT at 1.96 TeV (Tevatron) and 14 TeV (LHC14).

(4) $<p_T>$ versus the Multiplicity: "Min-Bias" and "Z-boson" Events

The total proton-antiproton cross section is the sum of the elastic and inelastic components, $\sigma_{tot} = \sigma_{EL} + \sigma_{IN}$. The inelastic cross section consists of three terms; single diffraction, double-diffraction, and everything else (referred to as the "hard core"), $\sigma_{IN} = \sigma_{SD} + \sigma_{DD} + \sigma_{HC}$. For elastic scattering neither of the beam particles breaks apart (*i.e.* color singlet exchange). For single and double diffraction one or both of the beam particles are excited into a high mass color

singlet state (*i.e.* N^* states) which then decays. Single and double diffraction also corresponds to color singlet exchange between the beam hadrons. When color is exchanged the outgoing remnants are no longer color singlets and one has a separation of color resulting in a multitude of quark-antiquark pairs being pulled out of the vacuum. The "hard core" component, σ_{HC}, involves color exchange and the separation of color. However, the "hard core" contribution has both a "soft" and "hard" component. Most of the time the color exchange between partons in the beam hadrons occurs through a soft interaction (*i.e.* no high transverse momentum) and the two beam hadrons "ooze" through each other producing lots of soft particles with a uniform distribution in rapidity and many particles flying down the beam pipe. Occasionally there is a hard scattering among the constituent partons producing outgoing particles and "jets" with high transverse momentum.

Minimum bias (*i.e.* "min-bias") is a generic term which refers to events that are selected with a "loose" trigger that accepts a large fraction of the inelastic cross section. All triggers produce some bias and the term "min-bias" is meaningless until one specifies the precise trigger used to collect the data. The CDF "min-bias" trigger consists of requiring at least one charged particle in the forward region $3.2 < \eta < 5.9$ and simultaneously at least one charged particle in the backward region $-5.9 < \eta < -3.2$. Monte-Carlo studies show that the CDF "min-bias" collects most of the σ_{HC} contribution plus small amounts of single and double diffraction [14].

Minimum bias collisions are a mixture of hard processes (perturbative QCD) and soft processes (non-perturbative QCD) and are, hence, very difficult to simulate. Min-bias collisions contain soft "beam-beam remnants", hard QCD 2-to-2 parton-parton scattering, and multiple parton interactions (soft & hard). To correctly simulate min-bias collisions one must have the correct mixture of hard and soft processes together with a good model of the multiple-parton interactions [M2]. The first model that came close to correctly modeling min-bias collisions at CDF was PYTHIA Tune A. Tune A was not tuned to fit min-bias collisions. It was tuned to fit the activity in the "underlying event" in high transverse momentum jet production [3]. However, PYTHIA uses the same p_T cut-off for the primary hard 2-to-2 parton-parton scattering and for additional multiple parton interactions. Hence, fixing the amount of multiple parton interactions (*i.e.* setting the p_T cut-off) allows one to run the hard 2-to-2 parton-parton scattering all the way down to $p_T(\text{hard}) = 0$ without hitting a divergence. For PYTHIA the amount of hard scattering in min-bias is, therefore, related to the activity of the "underlying event" in hard scattering processes. Neither HERWIG (without MPI) or HERWIG (with JIMMY MPI) can be used to describe "min-bias" events since they diverge as $p_T(\text{hard})$ goes to zero.

Fig. 3-15 shows CDF "min-bias" data corrected to the particle level at 1.96 TeV on the average p_T of charged particles versus the multiplicity for charged particles with $p_T > 0.4$ GeV/c and $|\eta| < 1$ from Ref. 14. The data are compared with PYTHIA Tune A, the PYTHIA ATLAS tune, and PYTHIA Tune A without MPI (pyAnoMPI). This is an important observable. The rate of change of $\langle p_T \rangle$ versus charged multiplicity is a measure of the amount of hard versus soft processes contributing to min-bias collisions and it is sensitive the modeling of the multiple-parton interactions [15]. If only the soft "beam-beam" remnants contributed to min-bias collisions then $\langle p_T \rangle$ would not depend on charged multiplicity. If one has two processes contributing, one soft ("beam-beam remnants") and one hard (hard 2-to-2 parton-parton scattering), then demanding large multiplicity will preferentially select the hard process and lead to a high $\langle p_T \rangle$. However, we see that with only these two processes $\langle p_T \rangle$ increases much too rapidly as a function of multiplicity (see pyAnoMPI). Multiple-parton interactions provides another mechanism for producing large multiplicities that are harder than the "beam-beam

remnants", but not as hard as the primary 2-to-2 hard scattering. PYTHIA Tune A gives a fairly good description of the $\langle p_T \rangle$ versus multiplicity, although not perfect. PYTHIA Tune A does a better job describing the data than the ATLAS tune. Both Tune A and the ATLAS tune include multiple-parton interactions, but with different choices for the color connections [16].

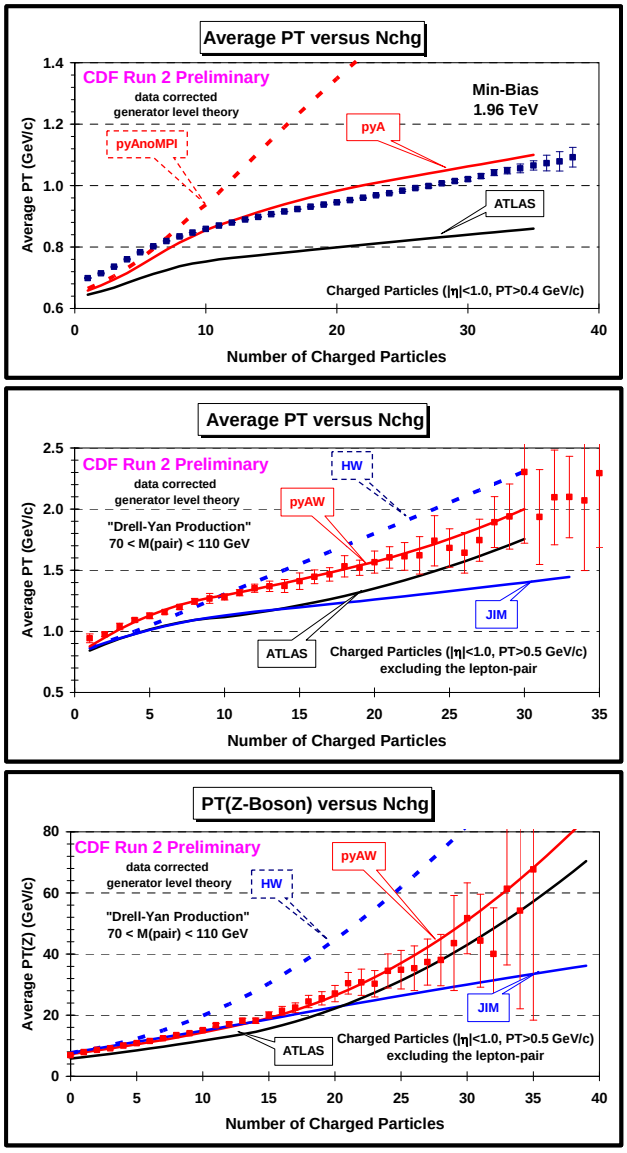

Fig. 3.15. (*top*) CDF "Min-Bias" data corrected to the particle level at 1.96 TeV on the average p_T of charged particles versus the multiplicity for charged particles with $p_T > 0.4$ GeV/c and $|\eta| < 1$ from Ref. 14. The data are compared with PYTHIA Tune A, the PYTHIA ATLAS tune, and PYTHIA Tune A without MPI (pyAnoMPI). (*middle*) Data corrected to the particle level at 1.96 TeV on the average p_T of charged particles versus the multiplicity for charged particles with $p_T > 0.5$ GeV/c and $|\eta| < 1$ for "Z-boson" events. (*bottom*) Data corrected to the particle level at 1.96 TeV on the average p_T of the Z-boson versus the multiplicity for charged particles with $p_T > 0.5$ GeV/c and $|\eta| < 1$ for "Z-boson" events. The "Z-boson" data are compared with PYTHIA Tune AW, the PYTHIA ATLAS tune, HERWIG (without MPI), and HERWIG (with JIMMY MPI).

Fig. 3-15 also shows the data corrected to the particle level at 1.96 TeV on the average p_T of charged particles versus the multiplicity for charged particles with $p_T > 0.5$ GeV/c and $|\eta| < 1$ for "Z-boson" events from this analysis. HERWIG (without MPI) predicts the $\langle p_T \rangle$ to rise too rapidly as the multiplicity increases. This is similar to the pyAnoMPI behavior in "min-bias" collisions. For HERWIG (without MPI) large multiplicities come from events with a high p_T Z-

boson and hence a large p_T "away-side" jet. This can be seen clearly in Fig. 3-15 which also shows the average p_T of the Z-boson versus the charged multiplicity. Without MPI the only way of getting large multiplicity is with high $p_T(Z)$ events. For the models with MPI one can get large multiplicity either from high $p_T(Z)$ events or from MPI and hence $<P_T(Z)>$ does not rise as sharply with multiplicity in accord with the data. PYTHIA Tune AW describes the data "Z-boson" fairly well.

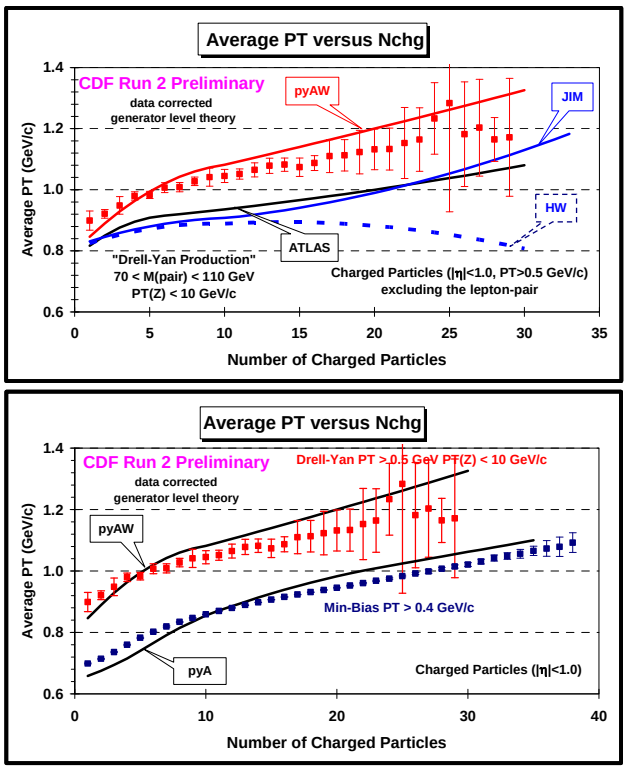

Fig. 3.16. (*top*) Data corrected to the particle level at 1.96 TeV on the average p_T of charged particles versus the multiplicity for charged particles with $p_T > 0.5$ GeV/c and $|\eta| < 1$ for "Z-boson" events in which $p_T(Z) < 10$ GeV/c. The data are compared with PYTHIA Tune AW, the PYTHIA ATLAS tune, HERWIG (without MPI), and HERWIG (with JIMMY MPI). (*bottom)* Comparison of the average p_T of charged particles versus the charged multiplicity for "Min-Bias" events from Ref. 14 with the "Z-boson" events with $p_T(Z) < 10$ GeV/c from this analysis. The "Min-Bias" data require $p_T > 0.4$ GeV/c and are compared with PYTHIA Tune A, while the "Z-boson" data require $p_T > 0.5$ GeV/c and are compared with PYTHIA Tune AW.

Fig. 3-16 shows the data corrected to the particle level at 1.96 TeV on the average p_T of charged particles versus the multiplicity for charged particles with $p_T > 0.5$ GeV/c and $|\eta| < 1$ for "Z-boson" events in which $p_T(Z) < 10$ GeV/c. We see that $<p_T>$ still increases as the multiplicity increases although not as fast. If we require $p_T(Z) < 10$ GeV/c, than HERWIG (without MPI) predicts that the $<p_T>$ decreases slightly as the multiplicity increases. This is because without MPI and without the high p_T "away-side" jet which is suppressed by requiring low $p_T(Z)$, large multiplicities come from events with a lot of initial-state radiation and the particles coming from initial-state radiation are "soft". PYTHIA Tune AW describes the behavior of $<p_T>$ versus the multiplicity fairly well even when we select $p_T(Z) < 10$ GeV/c.

Fig. 3-16 also shows a comparison of the average p_T of charged particles versus the charged multiplicity for "min-bias" events from Ref. 14 with the "Z-boson" events with $p_T(Z) < 10$ GeV/c. There is no reason for the "min-bias" data to agree with the "Z-boson" events with $p_T(Z) < 10$ GeV/c. However, they are remarkable similar and described fairly well by PYTHIA Tune

A and Tune AW, respectively. This strongly suggests that MPI are playing an important role in both these processes.

V. Summary & Conclusions

Observables that are sensitive to the "underlying event" in high transverse momentum jet production (*i.e.* "leading jet" events) and Drell-Yan lepton pair production in the mass region of the Z-boson (*i.e.* "Z-boson" events) have been presented and compared with several QCD Monte-Carlo model tunes. The data are corrected to the particle level and compared with the Monte-Carlo models at the at the particle level (*i.e.* generator level). The "underlying event" is similar for "leading jet" and "Z-boson" events as one would expect. The goal of this analysis is to provide data that can be used to tune and improve the QCD Monte-Carlo models of the "underlying event" that are used to simulate hadron-hadron collisions. The data presented here are also important for tuning the new QCD Monte-Carlo MPI models [15, 16].

PYTHIA Tune A and Tune AW do a good job in describing the data on the "underlying event" observables for "leading jet" and "Z-boson" events, respectively, although the agreement between theory and data is not perfect. The "leading jet" data show slightly more activity in the "underlying event" than PYTHIA Tune A. PYTHIA Tune AW is essentially identical to Tune A for "leading jet" events. All the tunes with MPI agree better than HERWIG without MPI. This is especially true in the "toward" region in "Z-boson" production. Adding JIMMY MPI to HERWIG greatly improves the agreement with data, but HERWIG with JIMMY MPI produces a charged particle p_T spectra that is considerably "softer" than the data. The PYTHIA ATLAS tune also produces a charged particle p_T spectra that is considerably "softer" than the data.

The behavior of the average charged particle p_T versus the charged particle multiplicity is an important observable. The rate of change of $\langle p_T \rangle$ versus charged multiplicity is a measure of the amount of hard versus soft processes contributing and it is sensitive the modeling of the multiple-parton interactions [16]. PYTHIA Tune A and Tune AW do a good job in describing the data on $\langle p_T \rangle$ versus multiplicity for "min-bias" and "Z-boson" events, respectively, although again the agreement between theory and data is not perfect. The behavior of $\langle p_T \rangle$ versus multiplicity is remarkable similar for "min-bias" events and "Z-boson" events with $p_T(Z) < 10$ GeV/c suggesting that MPI are playing an important role in both these processes.

Models with multiple-parton interactions like PYTHIA Tune DWT predict that the "underlying event" will become much more active (with larger $\langle p_T \rangle$) at the LHC. For HERWIG (without MPI) the "toward" region of "Z-boson" production does not change much in going from the Tevatron to the LHC. It is important to measure the "underlying event" observables presented here at the LHC. We will learn a lot about MPI by comparing the Tevatron results with the early LHC measurements.

References and Footnotes

1. T. Sjostrand, Phys. Lett. **157B**, 321 (1985); M. Bengtsson, T. Sjostrand, and M. van Zijl, Z. Phys. **C32**, 67 (1986); T. Sjostrand and M. van Zijl, Phys. Rev. **D36**, 2019 (1987). T. Sjostrand, P. Eden, C. Friberg, L. Lonnblad, G. Miu, S. Mrenna and E. Norrbin, Computer Physics Commun. **135**, 238 (2001). We use PYTHIA version 6.216.
2. *Hard Underlying Event Corrections to Inclusive Jet Cross-Sections*, Jon Pumplin, Phys. Rev. **D57**, 5787 (1998).

3. *Charged Jet Evolution and the Underlying Event in Proton-Antiproton Collisions at 1.8 TeV*, The CDF Collaboration (T. Affolder et al.), Phys. Rev. **D65**, 092002, (2002).

4. *Measurement of the Z PT Distribution in Proton-Antiproton Collisions at 1.8 TeV*, The CDF Collaboration (F. Abe et al.), Phys. Rev. Lett. **67**, 2937-2941 (1991).

5. The value of PARP(62), PARP(64), and PARP(91) was determined by CDF Electroweak Group. The "W" in Tune AW, BW, DW, DWT, QW stands for "Willis". I combined the "Willis" tune with Tune A, etc..

6. Phys. Rev. Lett. **94**, 221801 (2005).

7. J.M. Butterworth, J.R. Forshaw, and M.H. Seymour, Z. Phys. **C7**, 637-646 (1996).

8. G. Marchesini and B. R. Webber, Nucl. Phys **B310**, 461 (1988); I. G. Knowles, Nucl. Phys. B310, 571 (1988); S. Catani, G. Marchesini, and B. R. Webber, Nucl. Phys. **B349**, 635 (1991).

9. D. Acosta et al. (CDF Collaboration), Phys. Rev. **D71**, 032001 (2005); D. Acosta et al. (CDF Collaboration), Phys. Rev. **D71**, 052003 (2005); A. Abulencia et al. (CDF Collaboration), J. Phys. G Nucl. Part. Phys. **34**, (2007).

10. D. Acosta et al. (CDF Collaboration), Phys. Rev. Lett. **94**, 091803 (2005).

11. T. Aaltonen et al. (CDF Collaboration), Phys. Rev. Lett. **47**, 102001 (2008).

12. A. Affolder et al., Nucl. Instrum. Methods **A526**, 249 (2004).

13. The CDF Collaboration (A. Bhatti et al.), Nucl. Instrum. Meth, **A566**:375-412, 2006.

14. *Measurement of Particle Production and Inclusive Differential Cross Sections in Proton-Antiproton Collisions at 1.96 TeV*, N. Moggi et. al. (CDF Collaboration), CDF/PUB/MIN BIAS/PUBLIC/9550, *to be submitted to Phys. Rev. D*.

15. T. Sjostrand and P. Z. Skands, Eur. Phys. J., **C39** 129, (2005). T. Sjostrand, S. Mrenna and P. Skands, JHEP 05 (2006) 026.

16. P. Skands and D. Wicke, Eur. Phys. J. **C52** 133, (2007).